

Small x gluon from exclusive J/ψ production

A.D. MARTIN^a, C. NOCKLES^b, M. RYSKIN^{a,c} and T. TEUBNER^b

^a *Department of Physics and Institute for Particle Physics Phenomenology,
University of Durham, Durham DH1 3LE, U.K.*

^b *Department of Mathematical Sciences,
University of Liverpool, Liverpool L69 3BX, U.K.*

^c *Petersburg Nuclear Physics Institute, Gatchina, St. Petersburg, 188300, Russia*

Abstract

Exclusive J/ψ production, $\gamma^*p \rightarrow J/\psi p$, offers a unique opportunity to determine the gluon density of the proton in the small x domain. We use the available HERA data to determine the gluon distribution in the region $10^{-4} \lesssim x \lesssim 10^{-2}$ and $2 \lesssim Q^2 \lesssim 10 \text{ GeV}^2$, where the uncertainty on the gluon extracted from the global parton analyses is large. The gluon density is found to be approximately flat at the lower scale; it is compared with those of recent global analyses.

1 Introduction

Global analyses do not reliably determine the gluon for $x \lesssim$ a few 10^{-2} at low, yet perturbative, Q^2 as shown in Fig. 1. This is due partly to the lack of precise structure function data for $x \lesssim 10^{-4}$ and mainly due to the fact that the data included in global analyses actually probe the quark distribution, while the gluon density is constrained by the $\log Q^2$ dependence of the data, that is by the evolution. In the low x region the available Q^2 interval decreases and the accuracy of the gluon determination becomes worse. The strong dependence of the global fits for the gluon on the order of the analysis is clearly demonstrated in Fig. 1. Note that the recent

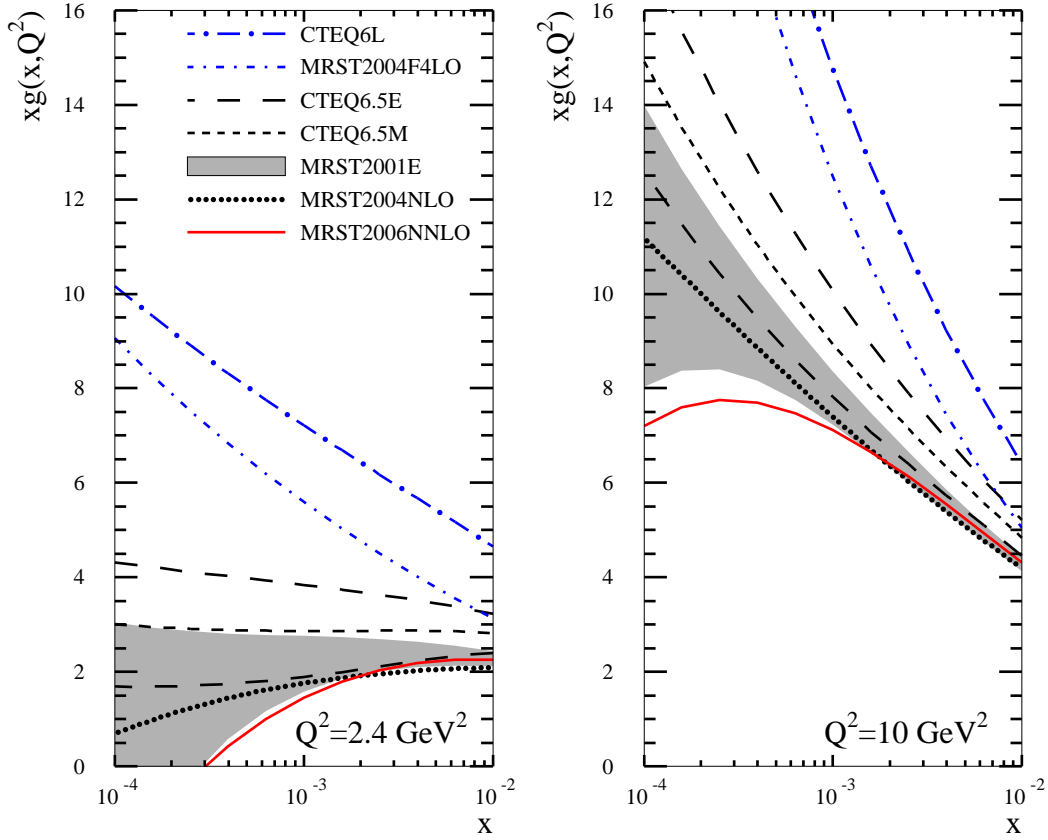


Figure 1: Comparison of recent global fits of the gluon distribution at small x at leading (LO), next-to-leading (NLO) and next-to-next-to leading (NNLO) order, for the two scales $Q^2 = 2.4$ (left) and 10 GeV^2 (right panel). LO gluons (dash dot) compared are CTEQ6L [1] and MRST2004F4LO [2]. The two (long) dashed lines indicate the error estimate of the CTEQ6.5 [3] gluon and the shaded band is the error band for the MRST2001 [4] global gluon. Central values for the NLO global fits are from CTEQ6.5M (short dashed) and MRST2004NLO [5] (dotted). The solid line represents MRST2006NNLO [6].

gluon from the MRST NNLO analysis [6] receives sizeable corrections both in size and shape compared to the NLO fit, signalling a large uncertainty of the gluon in this regime. In this context it is also interesting to note that the gluon as obtained from global fits can significantly change, both in normalisation and shape, if small x resummations are incorporated into the analysis [7].

Data for the exclusive $\gamma^*p \rightarrow J/\psi p$ process offer an attractive opportunity to determine the low x gluon density in this Q^2 domain, since here the gluon couples *directly* to the charm quark and the cross section is proportional to the gluon density *squared* [8]. Therefore the data are much more sensitive to the behaviour of the gluon. The mass of the $c\bar{c}$ vector meson introduces a relatively large scale, amenable to the perturbative QCD (pQCD) description not only of large Q^2 diffractive electroproduction, but also photoproduction of J/ψ . The available J/ψ data probe the gluon at a scale μ^2 in the range $2 - 10 \text{ GeV}^2$ for x in the range $10^{-4} \lesssim x \lesssim 10^{-2}$; that is just the domain where other data do not constrain the gluon reliably, see Fig. 1. It would be good to have comparable data on exclusive Υ production to determine the gluon at larger scales, but here the available data are sparse, see Fig. 5 below.

2 Exclusive J/ψ production at LO

To lowest order the $\gamma^*p \rightarrow J/\psi p$ amplitude can be factored into the product of the $\gamma \rightarrow c\bar{c}$ transition, the scattering of the $c\bar{c}$ system on the proton via (colourless) two-gluon exchange, and finally the formation of the J/ψ from the outgoing $c\bar{c}$ pair. The crucial observation is that at high γp centre-of-mass energy, W , the scattering on the proton occurs over a much shorter timescale than the $\gamma \rightarrow c\bar{c}$ fluctuation or the J/ψ formation times, see Fig. 2. Moreover, at leading logarithmic accuracy, this two-gluon exchange amplitude can be shown to be directly proportional to the gluon density $xg(x, \bar{Q}^2)$ with

$$\bar{Q}^2 = (Q^2 + M_{J/\psi}^2)/4, \quad x = (Q^2 + M_{J/\psi}^2)/(W^2 + M_{J/\psi}^2). \quad (1)$$

Q^2 is the virtuality of the photon and $M_{J/\psi}$ is the rest mass of the J/ψ . To be explicit, the lowest-order formula is [8]

$$\left. \frac{d\sigma}{dt}(\gamma^*p \rightarrow J/\psi p) \right|_{t=0} = \frac{\Gamma_{ee} M_{J/\psi}^3 \pi^3}{48\alpha} \left[\frac{\alpha_s(\bar{Q}^2)}{\bar{Q}^4} xg(x, \bar{Q}^2) \right]^2 \left(1 + \frac{Q^2}{M_{J/\psi}^2} \right), \quad (2)$$

where Γ_{ee} is the electronic width of the J/ψ .

In the leading logarithmic approximation, the integral over the transverse momentum k_T of the t -channel gluons, see Fig. 2, gives rise to the integrated gluon density $g(x, \bar{Q}^2)$. As usual in collinear factorisation, the k_T dependence of the integral is completely absorbed in the input gluon distribution (of the global analyses), taken at the factorisation scale \bar{Q}^2 . The integral over the charm quark loop is expressed in terms of the electronic width, Γ_{ee} , of J/ψ , and

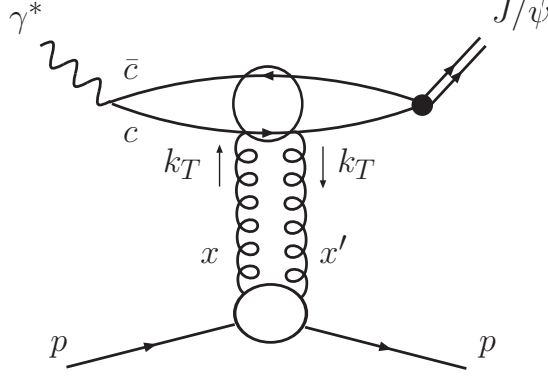


Figure 2: Schematic picture of high energy elastic J/ψ production, $\gamma^* p \rightarrow J/\psi p$. The factorised form follows since, in the proton rest frame, the formation time $\tau_f \simeq 2E_\gamma/(Q^2 + M_{J/\psi}^2)$ is much greater than the $c\bar{c}$ -proton interaction time τ_{int} . In the case of the simple two gluon exchange shown here, $\tau_{\text{int}} \simeq R$, where R is the radius of the proton.

the $Q^2/M_{J/\psi}^2$ term in the final brackets reflects the contribution of the longitudinally polarised incoming γ^* . Equation (2) gives the differential cross section at zero momentum transfer, $t = 0$. To describe data integrated over t , the integration is carried out assuming $\sigma \sim \exp(-bt)$ with b the experimentally measured slope parameter. Throughout this work the value

$$b = 4.5 \text{ GeV}^{-2} \quad (3)$$

is used, which is in agreement with [9, 10, 11].¹ Thus it becomes possible to extract the gluon density $g(x, \bar{Q}^2)$ directly from the measured diffractive J/ψ cross section.

3 Corrections to LO exclusive J/ψ production

Expression (2) is a simple, first approximation, justified in the LO collinear approximation using the non-relativistic J/ψ wave function. The relativistic corrections were intensively discussed in [12, 13]. The problem is that, simultaneously with the relativistic description of the c quarks, one needs to consider higher order Fock component $c\bar{c}g$ states of J/ψ . Hoodbhoy [14] has studied these two effects to order v^2/c^2 . He has shown that relativistic corrections to (2), written in terms of the experimentally measured Γ_{ee} , are small, $\sim \mathcal{O}(4\%)$, see [14]. So we do not account further for relativistic corrections below.

NLO corrections arise, first, from an explicit integration over the gluon k_T , which goes beyond the leading log contribution, arising from dk_T^2/k_T^2 , and, second, from more complicated

¹We neglect a slight energy dependence of b which is only observed for photoproduction, but which is of the order of differences between measurements of the two experiments H1 and ZEUS. The possible uncertainty is smaller than, or at most comparable to, other approximations used.

diagrams with one additional loop. To perform the explicit k_T integration we have to use the unintegrated gluon distribution, $f(x, k_T^2)$, which is related to the integrated gluon by

$$xg(x, \mu^2) = \int_{Q_0^2}^{\mu^2} \frac{dk_T^2}{k_T^2} f(x, k_T^2) + c(Q_0^2). \quad (4)$$

Of course, the infrared contribution cannot be treated perturbatively, and so we have introduced a lower limit Q_0^2 for the k_T^2 integral in the J/ψ production amplitude,

$$\left[\frac{\alpha_s(\bar{Q}^2)}{\bar{Q}^4} xg(x, \bar{Q}^2) \right] \longrightarrow \int_{Q_0^2}^{(W^2 - M_{J/\psi}^2)/4} \frac{dk_T^2 \alpha_s(k_T^2)}{\bar{Q}^2(\bar{Q}^2 + k_T^2)} \frac{\partial [xg(x, k_T^2)]}{\partial k_T^2} + \frac{\alpha_s(Q_0^2)}{\bar{Q}^4} xg(x, Q_0^2). \quad (5)$$

Expression (5) replaces the factor $\alpha_s(\bar{Q}^2)xg(x, \bar{Q}^2)/\bar{Q}^4$ in the LO result (2). To be precise, the unintegrated distribution f embodies the Sudakov factor $T(k_T^2, \mu^2)$ such that [15]

$$f(x, k_T^2) = \partial [xg(x, k_T^2)T(k_T^2, \mu^2)] / \partial \ln k_T^2. \quad (6)$$

Thus $c(Q_0^2)$ in Eq. (4) is given by $xg(x, Q_0^2)T(Q_0^2, \mu^2)$ and correspondingly for (5), $xg(x, Q_0^2) \rightarrow xg(x, Q_0^2)T(Q_0^2, \mu^2)$. In our numerics we have chosen $\mu^2 = \bar{Q}^2$. However, in the amplitude (5), the dominant contribution comes from the region of $k_T \sim \bar{Q}$ where $T(k_T^2, \mu^2)$ is close to unity. The inclusion of the T factor may be considered as an $\mathcal{O}(\alpha_s)$ correction to the gluon density and suppresses the gluon in our analysis by 1.7% for photoproduction at $x = 10^{-3}$. The contribution coming from $k_T < Q_0$ is written in terms of the integrated gluon $g(x, Q_0^2)$, that is the infrared part is absorbed into the input distribution at the ‘transition’ scale Q_0 .

Of course, at low Q^2 the gluon extracted from a global analysis may be affected by the presence of absorptive corrections which are usually neglected. Here, the absorptive corrections are expected to be smaller. The transverse size, r , of the $q\bar{q}$ dipole produced by the ‘heavy’ photon in DIS has a logarithmic distribution $\int dr^2/r^2$ starting from $1/Q^2$ up to some hadronic scale. In the case of J/ψ production the size of the $c\bar{c}$ dipole is limited by the size of the J/ψ meson. Even in photoproduction it is of the order of $1/\bar{Q}^2$. Since the probability of rescattering is proportional to r^2 , we anticipate a much smaller absorptive effect.

A more detailed analysis of the NLO corrections was done in [16, 17]. Part of these corrections generates the running of α_s , while part is similar to gluon Reggeization in the BFKL approach. Indeed, for J/ψ electroproduction it was shown [17] using the conventional collinear factorisation scheme, that there is a NLO correction of the form

$$\frac{3\alpha_s}{\pi} \ln\left(\frac{1}{x}\right) \ln\left(\frac{\bar{Q}^2}{\mu^2}\right). \quad (7)$$

In the k_T factorisation approach such a correction may be included by replacing the t -channel gluon by the Reggeized gluon. However this correction vanishes with a natural choice of the factorisation scale, $\mu^2 = \bar{Q}^2$, which was adopted in our prescription [18, 19, 15]. One therefore has reason to believe that the k_T factorisation approach accounts for a major part of the NLO

effect, and that the resulting ‘NLO’ gluon may be compared to that in a set of NLO global partons.² Therefore we shall refer to the resulting distributions as NLO gluons.

One also needs to account for the fact that the two gluons exchanged carry different fractions x, x' of the light-cone proton momentum, see Fig. 2. That is one has to use the generalised (skewed) gluon distribution.³ In our case $x' \ll x \ll 1$, and the skewing effect can be well estimated from [20]

$$R_g = \frac{2^{2\lambda+3} \Gamma(\lambda + \frac{5}{2})}{\sqrt{\pi} \Gamma(\lambda + 4)} \quad (8)$$

where $\lambda(Q^2) = \partial [\ln(xg)] / \partial \ln x$. That is in the small x region of interest we take the gluon to have the form $xg \sim x^{-\lambda}$.

Recall that the integral (5) was written for the discontinuity (i.e. for the imaginary part) of the amplitude shown in Fig. 2. The real part may be determined using a dispersion relation. In the low x region, for our positive-signature amplitude $A \propto x^{-\lambda} + (-x)^{-\lambda}$, the dispersion relation can be written in the form

$$\frac{\text{Re}A}{\text{Im}A} \simeq \frac{\pi}{2} \lambda \simeq \frac{\pi}{2} \frac{\partial \ln A}{\partial \ln(1/x)} \simeq \frac{\pi}{2} \frac{\partial \ln(xg(x, \bar{Q}^2))}{\partial \ln(1/x)}. \quad (9)$$

Both corrections lead to an enhancement of the cross section.

4 Determination of the gluon from J/ψ data

In the following, we present fits to the data for exclusive J/ψ production from HERA using the perturbative description discussed above.

In the low x region it is expected that the x dependence of the gluon density $xg(x, Q^2)$ is well approximated by the form $x^{-\lambda}$. However, the evolution in Q^2 modifies this behaviour, enlarging the power λ as Q^2 increases. In particular, in the double leading log (DLL) approximation, we have the asymptotic form

$$xg \sim \exp \left(\sqrt{\frac{4\alpha_s N_c}{\pi} \ln(1/x) \ln Q^2} \right). \quad (10)$$

²The global partons are defined in the $\overline{\text{MS}}$ regularization scheme. Our partons should also be considered to be in the $\overline{\text{MS}}$ scheme, since we use the $\overline{\text{MS}}$ definition of α_s , and moreover the factorisation scale which provides the cancellation of the $\alpha_s \ln 1/x$ correction is also specified in the $\overline{\text{MS}}$ scheme.

³In the formal analysis of the NLO contributions, there are effects arising from integrated quarks which generate gluons which then couple to the charm quark. In terms of our unintegrated gluon (f) description this should be considered as a NLO correction to the evolution of f . Since we do not consider the evolution, but just parametrise the scale dependence of the gluons (see below), this correction is outside our analysis.

Thus we need a Q^2 dependent parametrisation. However, in the limited region of Q^2 covered by the exclusive J/ψ data, it is sufficient to use a simple parametric form⁴

$$xg(x, \mu^2) = Nx^{-\lambda} \quad \text{with } \lambda = a + b \ln(\mu^2/0.45 \text{ GeV}^2). \quad (11)$$

The free parameters N , a and b are determined by a non-linear χ^2 fit to the exclusive J/ψ data from H1 [9] and ZEUS [11, 22].⁵ This three-parameter form provides enough flexibility to accurately describe the x and Q^2 behaviour of J/ψ production in the limited domain covered by the J/ψ data, namely $10^{-4} < x < 10^{-2}$ and $2 < Q^2 < 8 \text{ GeV}^2$, so we will use exactly Eq. (11) for the LO fit.

However, for the NLO approach, where we have the k_T^2 integral (5) which runs up to the kinematical limit $k_T^2 = (W^2 - M_{J/\psi}^2)/4$, we face the problem of a badly convergent k_T^2 integral. Indeed the low x gluons $xg \sim x^{-\lambda}$ obtain a large anomalous dimension γ . Since $x^{-b \ln k_T^2} = (k_T^2)^{b \ln(1/x)}$ we get $\gamma = b \ln(1/x)$. On the other hand, the expression (5) was calculated with running α_s . Recall that the scale dependence of the power λ was generated by the evolution of the form $\lambda = \int \alpha_s(q^2) \frac{dq^2}{q^2}$. Accounting for the running α_s , it is natural to replace the second term in the parametric form (11) by $\ln \ln(\mu^2/\Lambda_{\text{QCD}}^2)$. Therefore, for the NLO fit, we use

$$xg(x, \mu^2) = Nx^{-\lambda} \quad \text{with } \lambda = a + b \ln \ln(\mu^2/\Lambda_{\text{QCD}}^2). \quad (12)$$

The gluon densities obtained from the LO fit, using (2) with (11), together with the skewing and real part corrections, to the exclusive J/ψ data [9, 11, 22] are shown in Fig. 3.⁶ Inclusion of these corrections gives a 22% suppression of the gluon for photoproduction at $x = 10^{-3}$, with the skewing correction giving the dominant suppression of 18%. We use a 1-loop running α_s with $\alpha_s(M_Z^2) = 0.118$. In the analysis, error bands on the gluon and cross section are generated using the full covariance matrix for the fitted parameters, where as input we have added the statistical and systematic experimental errors of the data in quadrature. Compared to the gluons from the global fits, the gluon from our LO fit is similar in shape, but slightly smaller in normalisation and shows less rise towards smaller x with growing scales.

We now present the results of our NLO fit, which we obtain by modifying Eq. (2) by help of (5) with 2-loop running α_s , and replacing the parametrisation (11) by (12). Of course we also include skewing and real part corrections as before, and the T factor as discussed above. Figure 4 shows our fit using $Q_0^2 = 2 \text{ GeV}^2$ and $\Lambda_{\text{QCD}}^2 = 0.09 \text{ GeV}^2$. The dotted lines represent the central values of the gluons obtained using $Q_0^2 = 1 \text{ GeV}^2$. The NLO gluon fit shows a better matching to the global gluons at $x = 10^{-2}$ than the LO gluon obtained. The analysis

⁴Such a form has already successfully been used in [21] for the analysis of inclusive diffractive DIS data.

⁵We also performed fits for the data from the H1 and ZEUS collaborations separately. These fits typically have a smaller χ_{min}^2 , signalling a slight incompatibility between the data. However, they lead to similar results for the gluon. As the combined fit is very satisfactory ($\chi_{\text{min}}^2/\text{d.o.f.} < 1$), we will not discuss fits of individual data sets in the following.

⁶Note that in Figs. 3, 4 only a subset of 51 data points used in the fits is displayed, and there are data points at up to $\langle Q^2 \rangle = 22.4 \text{ GeV}^2$, corresponding to $\bar{Q}^2 = 8 \text{ GeV}^2$.

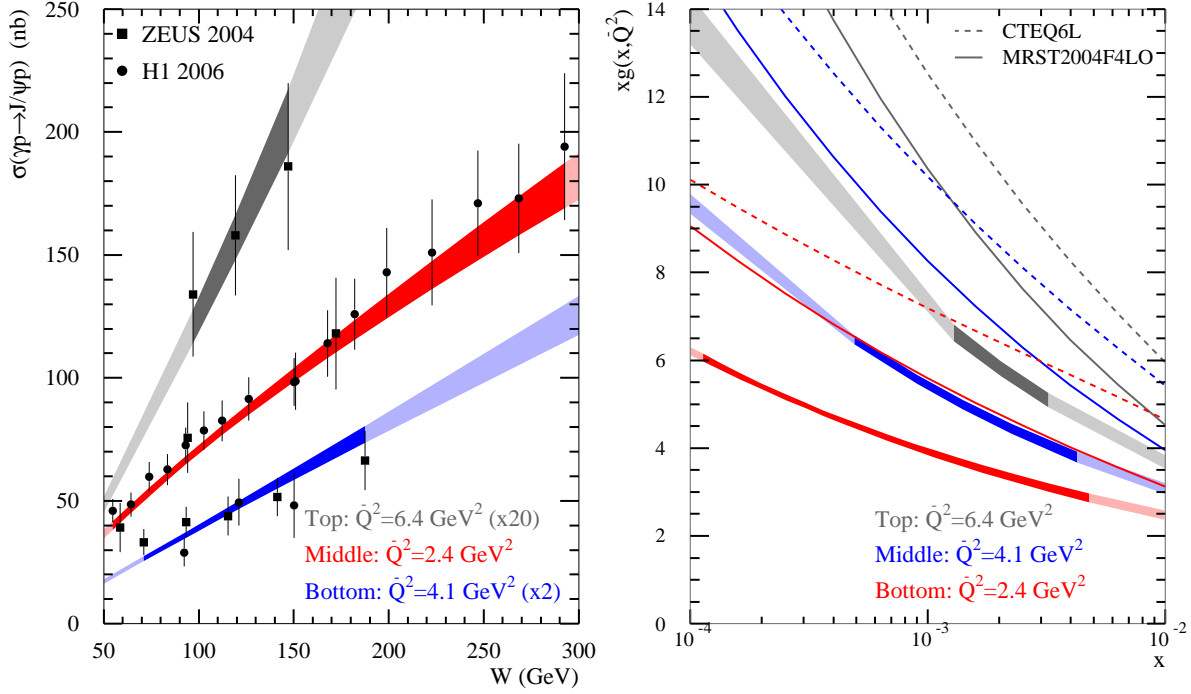


Figure 3: Leading order fit of elastic J/ψ data as described in the text. Left panel: cross section compared to some of the H1 [9] and ZEUS [11, 22] data, with values for \bar{Q}^2 as indicated; right panel: gluon compared to global fits for scales as indicated, where the solid (dashed) lines are the MRST2004F4LO [2] (CTEQ6L [1]) results. The width of the bands displays the uncertainty of the cross section and fitted gluon respectively, whereas the darker shaded areas indicate the region of the available data.

| | N | a | b | $\chi^2_{\min}/\text{d.o.f.}$ |
|-----|-----------------|-------------------|-------------------|-------------------------------|
| LO | 0.99 ± 0.09 | 0.051 ± 0.012 | 0.088 ± 0.005 | 0.9 |
| NLO | 1.55 ± 0.18 | -0.50 ± 0.06 | 0.46 ± 0.03 | 0.8 |

Table 1: Values of the three parameters of the LO and NLO gluon fits and corresponding $\chi^2_{\min}/\text{d.o.f.}$

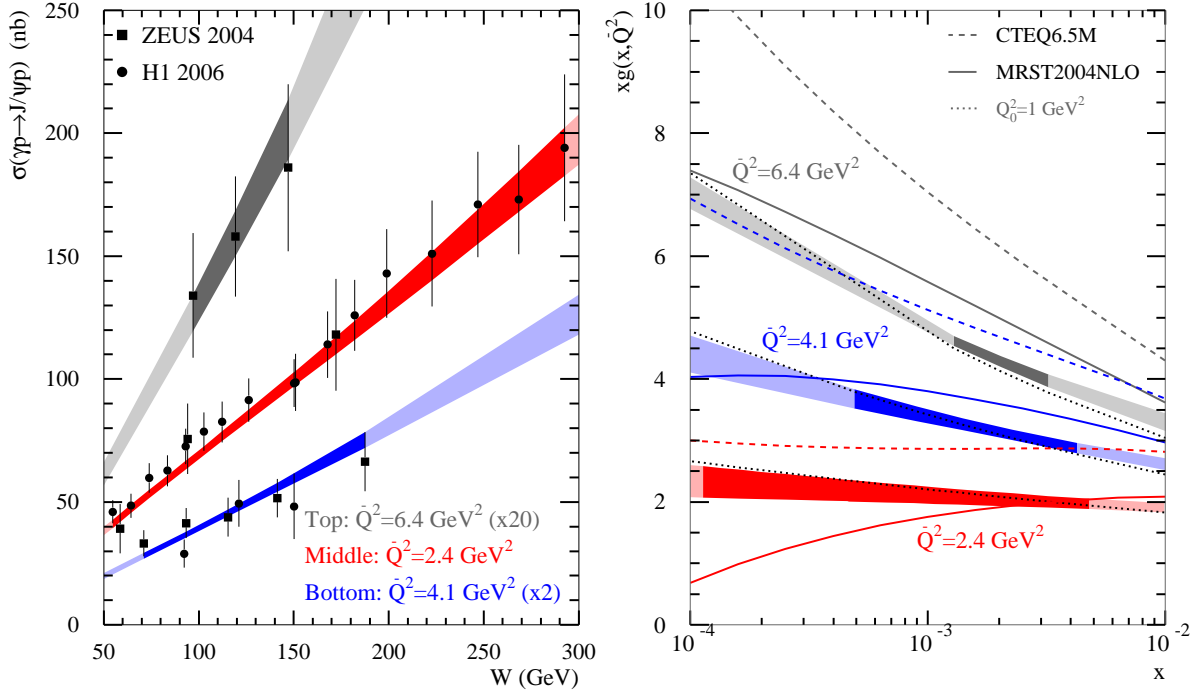


Figure 4: As Fig. 3, but for the next-to-leading order fit and comparing to NLO global fits from CTEQ6.5M [3] and MRST2004 [5].

| $Q^2(\text{GeV}^2)$ | $\lambda_{J/\psi}$ | λ_{MRST} | λ_{CTEQ} |
|---------------------|--------------------|--------------------------------|-----------------------------|
| 2.4 | 0.04 | $-0.17 \{-1.07, -0.16, 0.00\}$ | $0.01 \{0.04, 0.00, 0.05\}$ |
| 4.1 | 0.11 | $0.06 \{-0.03, 0.07, 0.16\}$ | $0.13 \{0.14, 0.13, 0.19\}$ |
| 6.4 | 0.16 | $0.15 \{0.09, 0.15, 0.24\}$ | $0.19 \{0.18, 0.19, 0.27\}$ |
| 8.0 | 0.19 | $0.18 \{0.13, 0.18, 0.27\}$ | $0.21 \{0.20, 0.22, 0.30\}$ |

Table 2: The values of the power of the gluon, λ , at four Q^2 values, for our NLO fit to elastic J/ψ production data compared to two global fits [3, 5]. The numbers for MRST and CTEQ are obtained through a fit in the range $x = 10^{-4} \dots 10^{-2}$, assuming $xg \sim x^{-\lambda}$ with an x independent λ , whereas the values in curly brackets are the logarithmic derivatives of the gluons at $x = \{10^{-4}, 10^{-3}, 10^{-2}\}$, respectively.

of the exclusive J/ψ data indicates that, at the larger scales, the small x behaviour of the gluon distribution is slightly flatter than that of the global analyses, both in their x behaviour and in their scale dependence of $\lambda(Q^2)$. At low scales, the gluon obtained from the J/ψ data still rises with decreasing x , especially in contrast to the MRST fit. For completeness we also present the values of the parameters for the LO and NLO fits (Tab. 1). As can be seen from Figs. 3, 4 and the $\chi^2_{\min}/\text{d.o.f.}$ values quoted in Tab. 1, our simple ansatz for the form of the gluon, $xg \sim x^{-\lambda}$, using an x independent power λ , works very well. To quantify the x and Q^2 behaviour, we tabulate the values of the power of the gluon, λ , from (12) at four Q^2 values, compared to values estimated from MRST2004NLO [5] and CTEQ6.5M gluons [3] (Tab. 2). As is evident from Fig. 4 and Tab. 2, our NLO gluon fit seems to be incompatible with the strength of evolution of the MRST global fit (e.g. at $x = 10^{-3}$ our gluon increases by a factor 2.7 from $Q^2 = 2.4$ to 8 GeV^2 compared to 3.7 for the MRST2004NLO gluon); however, there is fair agreement in the evolution between our gluon and the CTEQ fit (CTEQ evolves by a factor 2.8 in the same regime, although in absolute normalisation our NLO J/ψ prediction for the gluon agrees, on average, much better with the MRST NLO prediction). Of course, this should be seen in light of the large uncertainties of both the MRST and CTEQ gluons at small x and scales, see Figs. 1 and 4. This uncertainty persists at the largest scales probed in our fit. As these scales are rather low, the accuracy of the DGLAP approach may already be seriously affected by small x effects and absorptive and power suppressed corrections.

Of course, in the k_T factorisation approach there is some uncertainty arising from the infrared cut-off Q_0 , below which we cannot consider the k_T integration literally. We have to express this low k_T contribution in terms of the gluon integrated over k_T^2 up to Q_0^2 . However, with our prescription for unintegrated partons, these two contributions match smoothly to each other. The ambiguity due to the choice of Q_0 is quite small, as illustrated by the closeness of the dotted lines to our NLO gluons in Fig. 4.

Note that the difference between the LO and NLO gluons is large at the smallest x values, both in the global parton analyses and for the gluons obtained from elastic J/ψ production. For the global analyses this is due to the absence of the photon-gluon coefficient function at LO. At LO, the photon couples only to the quark parton, which is produced from a gluon at some scale $q^2 \ll Q^2$, due to the strong ordering in k_T . At low x the gluon grows with q^2 , and, to provide the measured values of the proton structure function F_2 , we need a much larger gluon distribution in the LO formalism. At NLO the photon-gluon coefficient function is present, which provides a direct photon-gluon parton coupling at the scale Q^2 , and, more importantly, a $1/x$ divergence appears in the quark-gluon splitting function, which accelerates the quark evolution and in turn requires less gluon. In elastic J/ψ production we have an analogous situation. By carrying out the k_T integration, we include the interaction with the gluon at large scales of the order of $Q^2 + M_{J/\psi}^2$. Moreover, part of this integral has $k_T^2 \gg Q^2$, and may be regarded as one step of backward evolution. In summary, in DGLAP analyses based on collinear factorisation, the large change in the gluon distribution in going from LO to NLO is due to the strong ordering in k_T and the absence of an additional loop integral in the LO coefficient function and parton evolution. Inclusion of higher-order terms beyond NLO is

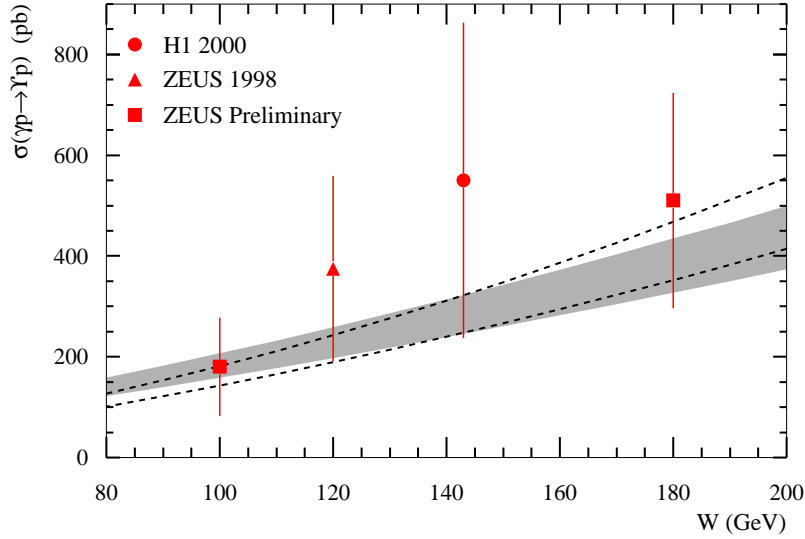


Figure 5: Prediction of elastic Υ photoproduction, using our LO and NLO gluon, compared to data. The dotted lines indicate the error band of the LO prediction, whereas the shaded band is our NLO prediction. The data points are the published ZEUS [23] and H1 [24] results, and the preliminary results from ZEUS [25].

expected to give a much smaller effect. They will mainly affect the normalisation and not the x dependence of the gluon.

The higher-order corrections in our approach are $\mathcal{O}(\alpha_s)$, but may be enhanced by large logarithms. The corrections which are enhanced by $\ln(1/x)$, and which may lead to some x dependence, are absorbed in the form of the gluon distribution by choosing the appropriate factorisation scale $\mu^2 = \bar{Q}^2$, see Eq. (7). Then, in our NLO approach, the part of the k_T integral which may be logarithmically large, is accounted for explicitly in the k_T factorisation formalism which is used to obtain the k_T integral. After this, those higher-order corrections, which are not included in the k_T integral, are concentrated in the domain $k_T \sim \mu = \bar{Q}$. Thus the scale dependence of these higher-order corrections is driven mainly by the scale dependence of the running of α_s which we take into account. The fact that the gluons obtained from our analysis turn out to be close to the gluon distributions coming from the global analyses for $x \simeq 10^{-2}$, where they are fairly stable, indicates that the omitted higher-order corrections are indeed small.

We have extended our framework to predict elastic Υ photoproduction, using our LO and NLO gluon with our cross section formulae including corrections and T factor, see Fig. 5. Although the data is sparse, the cross section predictions are reasonable.

We conclude that this new information coming from our NLO analysis of elastic J/ψ production data, in which the $c\bar{c}$ couple *directly* to the low x gluon parton and where the cross

section is proportional to the *square* of the gluon, is especially valuable to constrain the small x behaviour of the gluon distribution. The accuracy of the elastic J/ψ data is now sufficient, as indicated by the error bands (arising from the experimental uncertainties) on the extracted gluon distribution shown in Fig. 4, to improve our knowledge of the gluon distribution at small x , $x \gtrsim 10^{-4}$, considerably. This is in comparison to the small x behaviour of the ‘global’ gluon distributions, which is not well constrained by the inclusive DIS structure function data.

Acknowledgements

We would like to thank Robert Thorne for valuable discussions. TT thanks the UK Science and Technology Facilities Council for an Advanced Fellowship. The work of MR was supported in part by the Federal Program of the Russian Ministry of Industry, Science and Technology, RSGSS-5788.2006.02.

References

- [1] CTEQ Collaboration, J. Pumplin *et al.*, JHEP **0207** (2002) 012.
- [2] A.D. Martin, W.J. Stirling and R.S. Thorne, Phys. Lett. **B636** (2006) 259.
- [3] CTEQ Collaboration, W.-K. Tung *et al.*, JHEP **0702** (2007) 053.
- [4] A.D. Martin, R.G. Roberts, W.J. Stirling and R.S. Thorne, Eur. Phys. J. **C28** (2003) 455.
- [5] A.D. Martin, R.G. Roberts, W.J. Stirling and R.S. Thorne, Phys. Lett. **B604** (2004) 61.
- [6] A.D. Martin, W.J. Stirling, R.S. Thorne and G. Watt, Phys. Lett. **B652** (2007) 292.
- [7] C.D. White and R.S. Thorne, Phys. Rev. **D75** (2007) 034005.
- [8] M.G. Ryskin, Z. Phys. **C37** (1993) 89.
- [9] H1 Collaboration, A. Aktas *et al.*, Eur. Phys. J. **C46** (2006) 585.
- [10] ZEUS Collaboration, S. Chekanov *et al.*, Eur. Phys. J. **C24** (2002) 345.
- [11] ZEUS Collaboration, S. Chekanov *et al.*, Nucl. Phys. **B695** (2004) 3.
- [12] M.G. Ryskin, R.G. Roberts, A.D. Martin and E.M. Levin, Z. Phys. **C76** (1997) 231.
- [13] L. Frankfurt, W. Koepf, M. Strikman, Phys. Rev. **D54** (1996) 3194.
- [14] P. Hoodbhoy, Phys. Rev. **D56** (1997) 388.
- [15] A.D. Martin, M.G. Ryskin and T. Teubner, Phys. Rev. **D62** (2000) 014022.

- [16] D.Yu. Ivanov, M.I. Kotsky and A. Papa, Eur. Phys. J. **C38** (2004) 195.
- [17] D.Yu. Ivanov, A. Schäfer, L. Szymanowski and G. Krasnikov, Eur. Phys. J. **C34** (2004) 297.
- [18] E.M. Levin, A.D. Martin, M.G. Ryskin and T. Teubner, Z. Phys. **C74** (1997) 671.
- [19] A.D. Martin, M.G. Ryskin and T. Teubner, Phys. Rev. **D55** (1997) 4329, Phys. Lett. **B454** (1999) 339.
- [20] K. Golec-Biernat, A.D. Martin, M.G. Ryskin and A.G. Shuvaev, Phys. Rev. **D60** (1999) 014015.
- [21] A.D. Martin, M.G. Ryskin and G. Watt, Eur. Phys. J. **C37** (2004) 285.
- [22] ZEUS Collaboration, J. Breitweg *et al.*, Z. Phys. **C75** (1997) 215; Eur. Phys. J. **C6** (1999) 603.
- [23] ZEUS Collaboration, J. Breitweg *et al.*, Phys. Lett. **B437** (1998) 432.
- [24] H1 Collaboration, C. Adloff *et al.* Phys. Lett. **B483** (2000) 23.
- [25] Results presented by I. Rubinsky at the HEP2007 conference in Manchester, July 2007.